Ionic Strength-Dependent Physicochemical Factors in Cytochrome c_3 Regulating the Electron Transfer Rate

Tomoaki Ohmura,* Haruki Nakamura,# Katsumi Niki,§ Michael A. Cusanovich,¶ and Hideo Akutsu§

*Advanced Technology Research Center, Mitsubishi Heavy Industries, Ltd., Yokohama 236-8515, Japan; #Biomolecular Engineering Research Institute, Suita 565-0874, Japan; §Department of Chemistry and Biotechnology, Yokohama National University, Yokohama 240-8501, Japan; and ¶Department of Biochemistry, University of Arizona, Tucson, Arizona 85721 USA

ABSTRACT The effect of ionic strength on the macroscopic and microscopic redox potentials and the heme environment of cytochrome c_3 from *Desulfovibrio vulgaris* Miyazaki F have been investigated by NMR and electrochemical methods. The redox potentials of this tetraheme protein are found to be ionic strength-dependent. Especially, the microscopic redox potentials of hemes 2 and 3 at the fourth reduction step increase significantly with increasing ionic strength, which is in contradiction to the theoretical expectation. The coordinated imidazole proton signals are unaffected by ionic strength. However, the methyl and propionate proton signals of hemes 1 and 4 showed significant ionic strength dependencies that are distinct from those for hemes 2 and 3. This heme classification is the same as that found in the ionic strength dependencies of the microscopic redox potentials at the fourth reduction step. Furthermore, the effect of ionic strength on the electrostatic potentials at the heme irons has been examined on the theoretical basis. The electrostatic potential at heme 4 changes up to 1 M ionic strength, which was not expected from the observations reported on cytochromes so far. These results are discussed in connection with the reported anomalous ionic strength dependency of the reduction rate of cytochrome c_3.

INTRODUCTION

The cytochromes c_3 (cyt c_3) have been the subject of extensive study because of the presence of four hemes in a small polypeptide (typically 107 amino acids), their low redox potentials, asymmetric surface charge distribution, and the possibility that they may have applications as bioelectronic devices (Nakahara et al., 1977; Kimura et al., 1979). The three-dimensional structures of several examples of cyt c_3, including that from *Desulfovibrio vulgaris* Miyazaki F (*Dv*MF), the subject of this study, have been reported (Pierrot et al., 1982; Higuchi et al., 1984; Morimoto et al., 1991; Matias et al., 1993, 1996). In addition, a substantial amount of literature exists on the electrochemistry of cyt c_3 including the measurement of four macroscopic and 32 microscopic redox potentials for cytochrome c_3 (Santos et al., 1984; Gayda et al., 1988; Benosman et al., 1989; Fan et al., 1990; Coleta et al., 1991; Turner et al., 1994; Park et al., 1996). The macroscopic redox potentials are typically −240, −297, −315, and −357 mV vs. SHE at low ionic strength for *Dv*MF cyt c_3 (Niki et al., 1984). The large difference in apparent redox potential among the four identically ligated hemes appears to result in part from their local environments and in part from the effect of the oxidation state of nearby hemes.

All four hemes in *Dv*MF cyt c_3 have been identified by ^{1}H-NMR and related to their position in the amino acid sequence and three-dimensional structure. Thus, numbering the hemes by the position of the relevant cysteine residues in the amino acid sequence relative to the N-terminus, heme 4 is mainly reduced at the first reduction step, then followed by heme 1, heme 2, and finally heme 3 (Park et al., 1996). Because of the asymmetric surface charge distribution, the surfaces in the vicinity of the exposed heme edges of hemes 1 and 4 are positively charged, while the other two hemes have their exposed heme edges in primarily neutral environments (Higuchi et al., 1984).

The electron transfer kinetics of cyt c_3 have been studied in a number of laboratories in an effort to understand the mechanism of electron transfer by cyt c_3 (Tabushi et al., 1983; Haladjian et al., 1987; Sagara et al., 1991; Catarino et al., 1991; Akutsu et al., 1992). We have reported on the reduction kinetics of cyt c_3 by 5-deazariboflavin semiquinone, methylviologen cation radical, and reduced propylene diquat (Akutsu et al., 1992). These studies established that the cyt c_3 from *Desulfovibrio vulgaris* Hildenborough (*Dv*H) and *Dv*MF have rate constants which qualitatively depend on redox potential (driving force) as expected for outer sphere electron transfer. Moreover, individual cyt c_3 hemes have been analyzed in terms of their reduction kinetics (Akutsu et al., 1992). Since the sequence homology is 86%, the qualitative results were similar to each other for *Dv*H and *Dv*MF cyt c_3. As found with other redox proteins, for example, class I *c*-type cytochromes and high potential iron sulfur proteins, both electrostatics and the structure in the region of the exposed heme edge appear to modulate the reduction kinetics. However, during the course of the studies outlined above, it was found that the behavior of cyt c_3

Received for publication 26 January 1998 and in final form 28 May 1998.

Address reprint requests to Prof. Hideo Akutsu, Department of Chemistry and Biotechnology, Yokohama National University, Hodogaya-ku, Yokohama 240-8501, Japan. Tel.: +81-45-339-4232; Fax: +81-45-339-4251; E-mail: akutsu@bio.bsk.ynu.ac.jp.

Katsumi Niki's present address is Department of Chemistry, Iowa State University, Ames, IA 50011.

0006-3495/98/09/1483/08 $2.00

was anomalous by three different criteria. First, the reduction by the neutral deazariboflavin semiquinone was ionic strength-dependent, a result neither expected nor observed with other redox proteins. Second, a plot of the rate constant of reduction of cyt c_3 by reduced methylviologen, a cationic reductant, did not level off at high ionic strengths (>300 mM) in contrast with other redox proteins. In fact, the rate constant significantly increased above 250 mM ionic strength. Third, preliminary NMR experiments suggested that the chemical shift of heme methyl resonances was ionic strength-dependent (Akutsu et al., 1992).

Based on the ionic strength effects mentioned above, we proposed that high ionic strength resulted in a change in cyt c_3 redox potentials and/or structure (Akutsu et al., 1992). In the following we will report detailed studies on the effect of ionic strength on the redox potentials and structure of *Dv*MF cyt c_3.

MATERIALS AND METHODS

Cytochrome c_3 was purified from *Desulfovibrio vulgaris* Miyazaki F as previously described (Fan et al., 1990). Hydrogenase was added to a 3 mM cyt c_3 solution (molar ratio ~0.001) for NMR experiments to facilitate reduction. The extent of reduction of the cyt c_3 solution was controlled by the ratio of hydrogen and argon gasses in the NMR tube. All experiments were carried out in 30 mM potassium phosphate buffer (D_2O), p^{2}H 7.0 at 30°C. Ionic strength was controlled by addition of appropriate amounts of NaCl. The p^{2}H values reported are the direct pH meter readings.

^{1}H-NMR spectra were obtained with a Bruker AM400 NMR spectrometer. Chemical shifts are presented in parts per million relative to an internal standard of 2,2-dimethyl-2-silapentane-5-sulfonate (DSS). Saturation-transfer experiments were carried out for intermediate redox stages in order to assign heme methyl resonances for the five macroscopic oxidation states (Fan et al., 1990).

Differential pulse polarograms (DPP) were obtained using a dropping mercury electrode with a potentiostat, Fuso polarograph Model 312. The modulation amplitude, sweep rate, drop time, and sampling times were 10 mV, 2 mV/s, 2 s, and 20 ms, respectively. Cyt c_3 concentrations for differential pulse polarography were typically 0.1 mM. The formal potentials presented in this report are referred to the standard hydrogen electrode (SHE) at 30°C.

The electrostatic potentials at the heme irons were calculated by solving Poisson-Boltzmann equations in aqueous solvent (Nakamura and Nishida, 1987). The dielectric constant of the protein was assumed to be 2.0. All coordinated histidine residues are assumed to be neutral. Since the pK_a of His-67 is 8.6 (Park et al., 1991), it is cationic at pH 7.0. Heme (III) partial charges are used according to the reported ones (Saito and Kashiwagi, 1985a, b). The Debye shielding factor (κ) can be described as a function of ionic strength (I). Namely,

$$\kappa = (8\pi\epsilon e^2 N_A/1000\, k_B T)^{1/2}(I/e)^{1/2} \quad (1)$$

$$\epsilon = 78.5\text{–}14.0\, I \text{ (at } T = 300\ K) \quad (2)$$

where e, N_A, k_B, T, and ϵ are elementary charge, Avogadro constant, Boltzmann constant, absolute temperature, and dielectric constant of solvent, respectively (Takahashi et al., 1992). Contributions of individual residues to the electrostatic potential at each heme iron were analyzed using the Green's reciprocity theorem (Takahashi et al., 1992).

RESULTS

Macroscopic and microscopic redox potentials as a function of ionic strength

Cytochrome c_3 has five macroscopic oxidation states: S_0, S_1, S_2, S_3, and S_4 corresponding to the fully oxidized state, the one-electron, two-electron, three-electron, and fully reduced states, respectively. The macroscopic redox potentials E^j (j = I–IV, indicating the reduction step), of *Dv*MF cyt c_3 were determined by least-squares fitting of the differential pulse polarograms to the analytical equations for the four consecutive one-electron reversible electrode reactions (Niki et al., 1984) at seven ionic strengths ranging from 53 to 1023 mM. Fig. 1 is a graphic representation of the apparent macroscopic redox potentials as a function of the square root of ionic strength. The use of the square root of the ionic strength does not have any theoretical meaning under the conditions used here, but does provide a convenient way to present the ionic strength effect. Within experimental error, E^I is independent of ionic strength; E^{II} and E^{III} show small increases with increasing ionic strength, while E^{IV} has a relatively large (22 mV over the ionic strength range 53–1023 mM) positive correlation with increasing ionic strength. The situation becomes much clearer with the microscopic redox potentials.

The redox potential of each heme in a defined oxidation state (the microscopic redox potential, e_i^j) and interacting potentials ($I_{ii'}$) can be estimated by the use of the reduced fractions (R_i^j) determined from the chemical shifts of the heme methyl NMR signals and the macroscopic redox potentials (Fan et al., 1990). Here, the subscript and superscript stand for the heme number and the reduction step, respectively. In the case of *Dv*MF and *Dv*H cyt c_3, the microscopic redox potentials were shown to be pH dependent in the neutral pH region because of the carboxyl group of heme 1 (Park et al., 1996; Turner et al., 1996). Since the pK_a of the carboxyl group depends on the oxidation state,

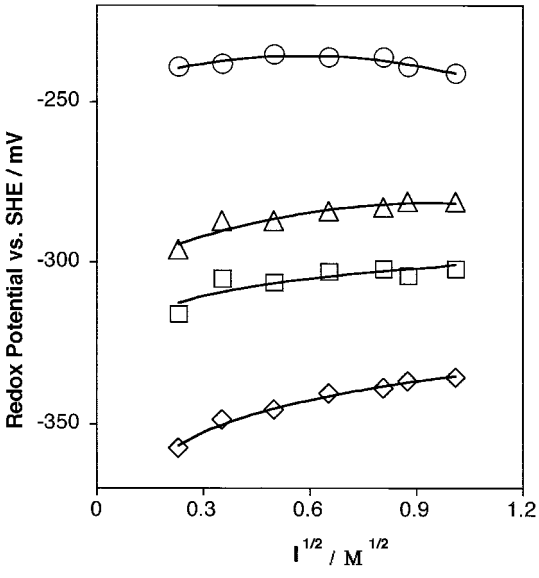

FIGURE 1 Macroscopic redox potentials of *Dv*MF cytochrome c_3 as a function of the square root of the ionic strength at p^{2}H 7.0 and 30°C. Circles, triangles, squares, and lozenges denote E^I, E^{II}, E^{III}, and E^{IV}, respectively. SHE and E^j (j = I–IV) denote the standard hydrogen electrode and the macroscopic redox potential at the jth reduction step, respectively.

the interacting potentials would depend on the oxidation state. This would give the ambiguity to the calculation of the interacting potentials (Turner et al., 1996). However, e_i^I and e_i^{IV} can be determined directly from the macroscopic redox potentials and the reduced fractions R_i^I and R_i^{IV} at given pH (Fan et al., 1990). Namely,

$$e_i^I = E^I + (RT/F) \ln R_i^I \quad (3)$$

$$e_i^{IV} = E^{IV} - (RT/F) \ln R_i^{IV} \quad (4)$$

where E^j, R, T, and F stand for the macroscopic redox potential at the jth reduction step, gas constant, absolute temperature, and Faraday constant, respectively. Thus, there is no ambiguity in determining e_i^I and e_i^{IV}. By using this approach, the microscopic redox potentials for the first and fourth reduction steps were determined at various ionic strengths in the range from 53 to 1023 mM. The chemical shifts of the heme methyl signals in the five oxidation states at 53 and 1023 mM ionic strength (the extremes studied) are presented in Table 1 for each of the oxidation states. In general, the chemical shift decreased on going from S_0 to S_4. The individual heme methyl resonances (labeled A–J from the low field to high field) were assigned for individual hemes (hemes 1–4) as previously described (Park et al., 1996). In the table both the letter notation and specific assignments in terms of porphyrin nomenclature recommended by IUPAC-IUB are given. Fig. 2 presents the effect of ionic strength on individual methyl resonances for the fully oxidized protein. Note that ionic strength has a generally similar effect on hemes 1 and 4, which is distinct from that found for hemes 2 and 3, although they behave similarly. Moreover, the chemical shift of the methyl resonance of J of heme 3 behaved significantly differently from other heme methyl signals at low ionic strength. At 53 mM ionic strength, the chemical shifts of J for S_1 and S_3 were larger than those for S_0 and S_2, respectively. This was interpreted in terms of the pseudocontact shifts induced by adjacent hemes (Salgueiro et al., 1997). At 1023 mM ionic strength, however, this abnormality was significantly eased, suggesting that a structural change induced by the electrostatic interactions is also involved in the unusual redox behavior of signal J.

Table 2 summarizes the microscopic redox potentials for the first and fourth reduction steps as a function of ionic

TABLE 1 Chemical shifts (ppm) of heme methyl signals for the five macroscopic oxidation states, at 53 mM and 1023 mM ionic strength, 30°C and p^{2}H 7.0

Signals	Oxidation States				
	S_0	S_1	S_2	S_3	S_4
Ionic strength 53 mM					
Heme 1					
18^1 CH_3 (B)	29.31	26.97	13.06	4.90	3.25
2^1 CH_3 (F)	18.98	17.70	9.73	4.16	3.26
12^1 CH_3 (G)	18.07	17.26	8.83	3.78	3.29
Heme 2					
18^1 CH_3 (C)	20.51	19.83	16.37	6.66	3.15
7^1 CH_3 (D)	20.24	19.30	14.75	6.03	3.16
Heme 3					
12^1 CH_3 (E)	19.90	16.88	13.46	13.02	3.47
2^1 CH_3 (J)	13.52	13.86	11.45	12.10	4.68
Heme 4					
18^1 CH_3 (A)	30.51	12.11	10.81	7.57	3.23
2^1 CH_3 (H)	17.53	7.60	6.77	5.45	3.18
Ionic strength 1023 mM					
Heme 1					
18^1 CH_3 (B)	29.14	25.93	12.80	5.21	3.34
2^1 CH_3 (F)	19.33	17.65	9.94	4.59	3.04
Heme 2					
18^1 CH_3 (C)	20.46	19.76	15.67	6.77	3.29
7^1 CH_3 (D)	20.19	19.08	14.07	6.28	3.35
Heme 3					
12^1 CH_3 (E)	19.84	15.53	12.87	11.56	3.58
2^1 CH_3 (J)	13.54	12.01	10.50	10.47	4.62
Heme 4					
18^1 CH_3 (A)	30.39	15.32	13.51	10.35	3.36

S_j denotes the j-electron reduced state. Hemes are numbered according to the sequence. Letter notations for the signals are given in the parentheses.

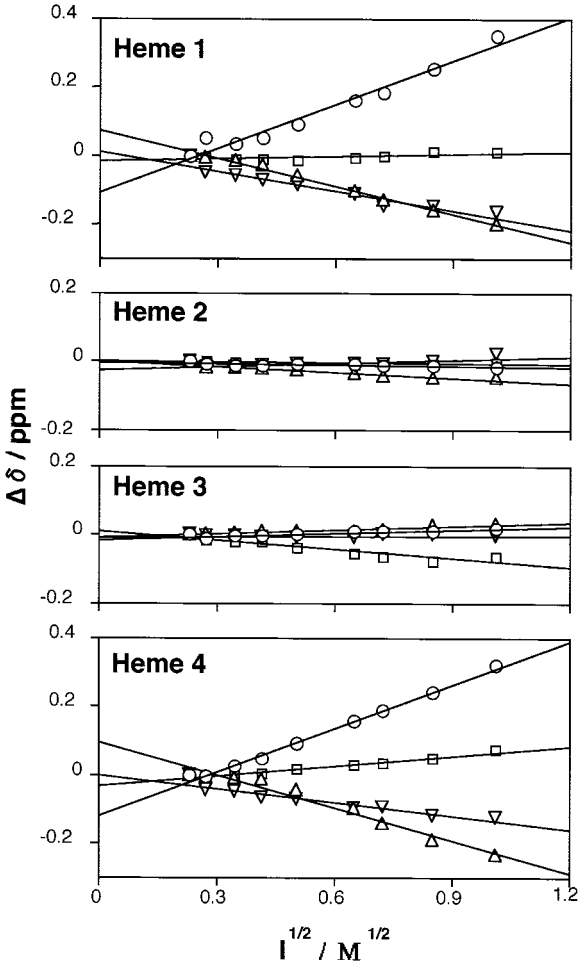

FIGURE 2 Chemical shift changes of the heme methyl resonances ($\Delta\delta$) of *Dv*MF cytochrome c_3 as a function of the square root of the ionic strength. The heme numbering is according to the amino acid sequence. Circles, triangles, squares, and inverse triangles represent 2^1 CH_3, 7^1 CH_3, 12^1 CH_3, and 18^1 CH_3 signals, respectively.

TABLE 2 The microscopic redox potentials (mV) for the first and fourth reduction step (e_i^I and e_i^{IV}, respectively).

Potentials (mV)	Ionic strength (mM)				
	53	253	423	653	1023
e_1^I	−307 (3)	−301 (3)	−301 (4)	−295 (2)	−298 (3)
e_2^I	−319 (6)	−313 (5)	−315 (7)	−313 (5)	−317 (5)
e_3^I	−282 (2)	−277 (2)	−275 (2)	−271 (1)	−275 (1)
e_4^I	−249 (1)	−245 (1)	−248 (1)	−250 (1)	−256 (1)
e_1^{IV}	−280 (5)	−274 (4)	−268 (5)	−265 (3)	−271 (3)
e_2^{IV}	−314 (2)	−303 (1)	−297 (2)	−293 (1)	−292 (2)
e_3^{IV}	−345 (1)	−331 (1)	−326 (1)	−321 (1)	−316 (1)
e_4^{IV}	−310 (2)	−301 (2)	−297 (2)	−295 (1)	−301 (2)

Standard deviations are given in parentheses. Sequential heme numbering is used in the subscripts for the potential notations.

strength as derived from the macroscopic potentials and NMR data. It was indicated that the best choice to determine the redox potentials of *Dv*H and *Dv*MF cyt c_3 are signals A, B, D, and E because these methyl groups are located on the surface of the protein in the crystal structures (Turner et al., 1994; Salgueiro et al., 1997). This may be correct for the first approximation, but the situation is not simple. For example, the chemical shift of signal E of *Dv*H cyt c_3 behaves abnormally during the reduction (or oxidation) between S_2 and S_3 states (Turner et al., 1994) despite its location on the protein surface. The abnormality of signal E was eased at a high ionic strength (1023 mM) (Park et al., 1997). We have also compared the microscopic redox potentials obtained from the chemical shifts of signals A, B, D and E with those from signals A–H at 53 mM ionic strength. The differences were within the standard deviations obtained from the chemical shifts of signals A–H. Therefore, we used the chemical shifts of as many signals as possible in this work for the calculation. Signal J was not included in the calculation because of its significant abnormality.

The profiles of the microscopic redox potentials at the first and last reduction steps are presented as a function of the square root of the ionic strength in Fig. 3. In general, the tendency was similar to that of the macroscopic redox potentials. In the case of e_i^I, three of four potentials increased with increasing ionic strength (2–9 mV) and one (e_4^I) decreased, being consistent with the overall observation of E^I. In contrast, all values of e_i^{IV} increased with increasing ionic strength (9–29 mV) consistent with the large increase of E^{IV} with increasing ionic strength.

The effect of ionic strength on the chemical shifts of the coordinated histidine imidazole and heme propionate groups of ferricytochrome c_3

It was shown that the C2 proton signals of the coordinated imidazoles of cyt c_3 appear in the extremely high field region in the fully oxidized state (Akutsu and Hirasawa, 1992). The ionic strength dependence for all eight coordinated histidine C2 protons was examined for the ionic strength range from 53 to 1223 mM. No effect of ionic

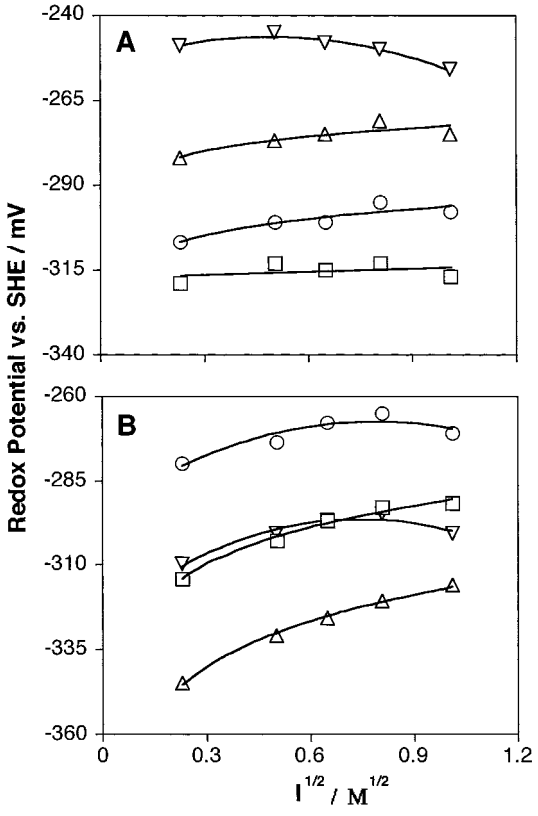

FIGURE 3 Microscopic redox potentials of *Dv*MF cytochrome c_3 for the first and fourth reduction steps as a function of the square root of the ionic strength at p^2H 7.0 and 30°C. SHE and e^j_i (j = I–IV) denote the standard hydrogen electrode and microscopic redox potential of heme i at the *j*th reduction step, respectively. (*A*) First reduction step; (*B*) fourth reduction step. Circles, squares, triangles, and inverse triangles represent hemes 1–4, respectively.

strength on the C2 protons was observed, suggesting that there is no alteration in the coordination structure in the four hemes.

The chemical shift changes of the propionate methylenes (13^{1a} CH_2, 13^{1b}, CH_2) of the fully oxidized protein were measured and are plotted as a function of the square root of the ionic strength in Fig. 4. They were unambiguously assigned through the NOE in one-dimensional spectra in which the 12^1 methyl signal was irradiated. The profiles for the propionate methylenes were similar to those for the heme methyl groups. Namely, those of hemes 1 and 4 are clearly ionic strength-dependent, while the chemical shift changes of those of hemes 2 and 3 have a relatively small ionic strength dependence, with the exception of heme 3 at very high ionic strengths.

Estimation of the electrostatic potentials at the heme irons

The electrostatic potentials at the heme irons of *Dv*MF cyt c_3 were calculated at the ionic strength 0, 50, 100, 300, 600, and 1000 mM. At zero ionic strength, the electrostatic potentials at the irons of hemes 1–4 were −113, −383,

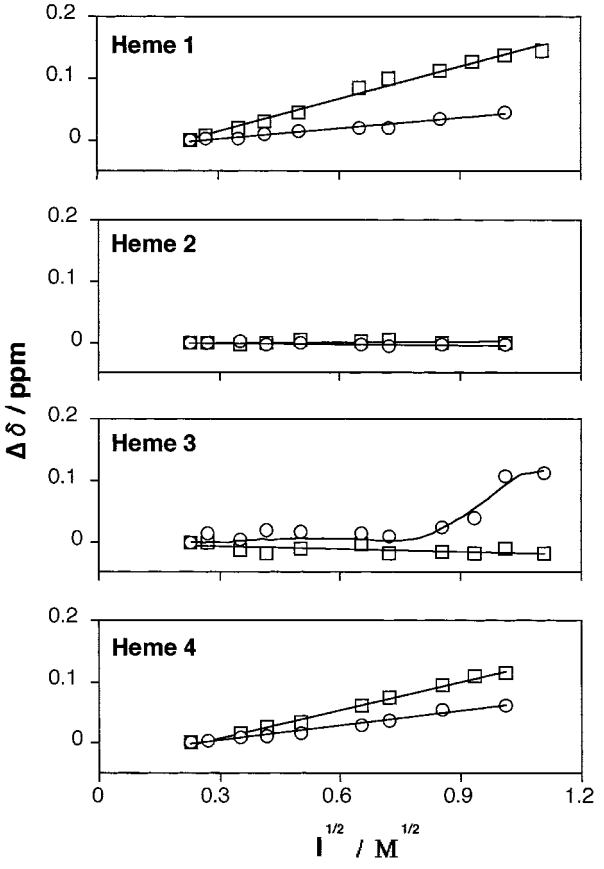

FIGURE 4 The chemical shift changes of 13^{1a} and 13^{1b} CH_2 resonances of *Dv*MF ferricytochrome c_3 as a function of the square root of the ionic strength at p^2H 7.0 and 30°C. The heme numbering is according to the amino acid sequence. The open circles and open squares represent the nonequivalent two protons of the propionate α-methylene groups.

−155, and −129 mV, respectively, with the effects of the other three hemes except their own hemes (a model of the fully oxidized cyt c_3). The propionates of their own hemes are included in the calculation. When no contribution from the hemes except propionates was included, they were −354, −588, −440, and −310 mV, respectively.

The absolute values of the estimated electrostatic potentials largely depend upon the dielectric constant inside the protein, which cannot be well defined in the calculations (Nakamura, 1996). However, the characteristic features of the potential distribution are qualitatively well explained by solving the Poisson-Boltzmann equations. From the current calculations with the effect of the other three hemes, the iron position of heme 1 has the highest electrostatic potential, followed by those of heme 4, heme 3, and heme 2. Except for heme 1, the order of those potentials corresponds well with the order of the e_i^I values in Table 2. Since heme 1 should strongly interact with heme 2, as revealed by the very large interacting potential I_{12} (Park et al., 1996), the e_1^I may decrease correlating with heme 2, which has the lowest electrostatic potential at the iron. This tendency of the absolute values of the electrostatic potential at individual iron positions did not change when calculations were performed with the high dielectric constant inside the protein (ϵ_p = 10) instead of 2 (data not shown).

The contributions of the individual protein residues to the above electrostatic potential at each heme iron were analyzed based upon the crystal structure. For heme 2, with the lowest electrostatic potential, carbonyl oxygens of Cys-33, Asp-42, Gln-44, and Cys-46 in the neighborhood of the heme 2 iron are unpaired with any other hydrogen bond donors. Moreover, carboxylates of the buried Asp-42 side chain and the heme 1 propionate are close to the position of the heme 2 iron. These factors make the potential of heme 2 very low. In contrast, heme 4 is surrounded by many cationic residues, such as Lys-15, Lys-57, Lys-58, Lys-60, His-67, Lys-72, and Lys-101, located on the molecular surface. Due to the negative contribution of the own propionates of heme 4, the absolute electrostatic potential has a negative value, but it is much higher than that of heme 2.

The electrostatic potentials at the heme irons at the ionic strengths mentioned above are plotted as the differences from those at zero ionic strength in Fig. 5, *A* and *B*, with and without the heme contributions, respectively. It is evident from Fig. 5 that the potential at the heme 4 iron significantly

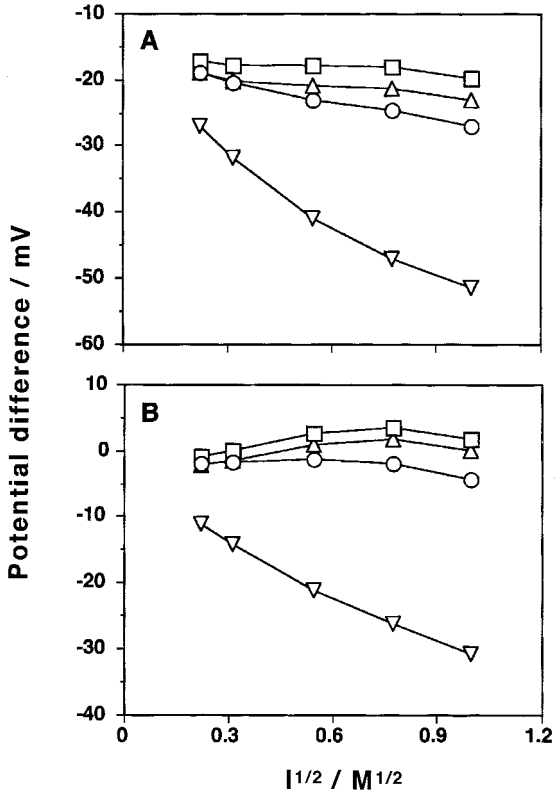

FIGURE 5 The calculated electrostatic potential at each heme iron of *Dv*MF cytochrome c_3 as the difference from that at zero ionic strength. Calculated are the potentials for 0, 50, 100, 300, 600, and 1000 mM ionic strengths. The potential at 0 mM ionic strength was subtracted from those at the other ionic strengths. Circles, squares, triangles, and inverse triangles represent hemes 1–4, respectively. (*A*) Calculated results considering the contribution from the other three hemes; (*B*) without the contribution of any hemes.

decreases with an increase of the ionic strength up to 1000 mM. This was not expected from the results on cytochromes reported so far. Furthermore, the potentials of hemes 2 and 3 behave similarly and are almost independent of ionic strength in the region from 50 to 1000 mM. To understand the contributions of the individual amino acid residues to the ionic strength dependency of the redox potentials e_i^I, the differences between the contributions of the residues to the electrostatic potential at each heme iron at 50 mM ionic strength and that at 1 M ionic strength were calculated on the basis of the crystal structure. They are presented in Fig. 6. A precise balance among the cationic and anionic residues determines the ionic strength dependency of the total electrostatic potential at each heme iron. In fact, in hemes 1 and 4, the positive contributions due to cationic residues surrounding the hemes are shielded at high ionic strength much more effectively than the negative ones due to fewer anionic residues. The unusual ionic strength dependency of the electrostatic potential at the heme 4 iron can be ascribed to the significantly high density of the positive charges around the heme. In contrast, in hemes 2 and 3, the effects from the cationic and anionic residues are nearly equal.

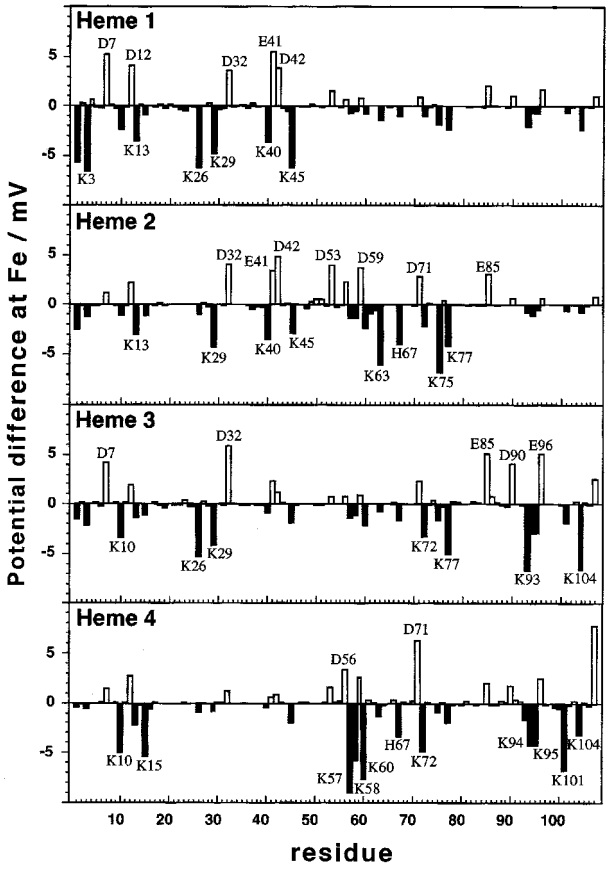

FIGURE 6 The contributions of the individual residues to the electrostatic potential at each heme iron of *Dv*MF ferricytochrome c_3 at 1 M ionic strength as the difference from that at 50 mM ionic strength. The potential at 50 mM ionic strength was subtracted from that at 1 M ionic strength. Black and white bars indicate the negative and positive contributions. The residues, which give significant contributions, are indicated by one-letter amino acid codes and residue numbers in the figure.

DISCUSSION

The results in this work provide an insight into the anomalous properties of the reduction kinetics of cyt c_3. Kinetic studies to date have focused on *Dv*H cyt c_3 with qualitatively similar results for *Dv*MF cyt c_3 (Akutsu et al., 1992) although it was not studied as extensively. Since the sequential homology is 86% and the crystal structures are almost identical for *Dv*H and *Dv*MF cyt c_3 (Higuchi et al., 1984; Morimoto et al., 1991; Matias et al., 1993), we can discuss the reduction kinetics of *Dv*H cyt c_3 on the basis of the physicochemical properties of *Dv*MF cyt c_3 obtained in this work. Three reactions have been studied: the reduction of cyt c_3 by deazariboflavin semiquinone ($DRFH^{\bullet}$, which is uncharged); one electron-reduced propylene diquat (PDQ^+, positively charged); and one electron-reduced methyl viologen (MV^+, positively charged). The latter two reductants were used to examine the electrostatic interaction between the reductant and cyt c_3, which is a basic protein.

In the cases of $DRFH^{\bullet}$ and PDQ^+, the kinetics were analyzed at two ionic strengths (low, 16 or 90 mM; high, 500 mM). The quantitative values of the rate constants are difficult to analyze because of the complexities of resolving four individual components and the fact that the microscopic redox potentials are different at different stages of reduction. Therefore, the reduction processes were analyzed using four reduction rates as a first approximation (Akutsu et al., 1992). Overall, the kinetics for PDQ^+ reduction increase with increasing ionic strength, being consistent with the neutralization of repulsive interactions (plus-plus) and with the increase in driving force due to the increase in the redox potentials of the cyt c_3 hemes as found in this work. In contrast, the rate constant for the first reduction (presumably the reduction of heme 4, the highest potential heme at the first reduction step) by $DRFH^{\bullet}$ decreases with increasing ionic strength and the fourth rate constant (presumably the reduction of heme 3, the lowest potential heme at the fourth reduction step) increases. Since $DRFH^{\bullet}$ is neutral, electrostatic interactions between the reactants should not be relevant. The increase of the fourth rate constant can be explained by the effect of increasing the driving force (e_3^{IV}) at high ionic strength. However, a small change of e_4^I cannot explain the decrease of the first rate constant. Apparently, steric or electronic effects result in a decrease in the reduction kinetics, which overshadow the driving force effect. This is supported by the observation on the chemical shifts of heme methyl and propionate signals (Figs. 2 and 4). Those of hemes 4 and 1 changed significantly depending on the ionic strength, although no changes were detected for the coordinated imidazole groups at different ionic strength. Therefore, the changes observed in the NMR signals should reflect alterations in the surrounding polypeptide or the solvent. Actually, one propionate group

is almost buried in the protein for hemes 4 and 1 according to the crystal structure of *Dv*MF cyt c_3 (Higuchi et al., 1984). Since they are expected to have a negative charge, the conformation around this carboxyl group would change depending on the ionic strength. Since hemes 4 and 1 are mainly reduced at the first and second reduction steps, respectively, this could be a major reason for the suppression of the electron transfer at the first stage of the reduction by $DRFH^{\bullet}$. Note that a similar process will be occurring in PDQ^+ and MV^+ reduction kinetics, which are masked by dominant electrostatic effects.

In the case of MV^+ reduction, only the overall reduction kinetics were measured (individual hemes were not resolved) and the ionic strength range was extended to 1 M. In this case, the measured rate constant increases (~ 3-fold) with increasing ionic strength over the ionic strength range 16–1000 mM. The increase in the rate constant appears to be leveling off in the 200–300 mM ionic strength range, but then strongly increases (~ 1.7-fold) between 250 and 1000 mM. The first part of the curve behaves as expected for the interaction of two positively charged reactants. However, the latter part is unusual. The estimation of the electrostatic potentials at the heme irons showed that while the effect of positive charges is suppressed at 100–300 mM ionic strength for hemes 1–3, as expected, the positive charges around heme 4 cannot be shielded by the ionic strength up to 1000 mM (Fig. 5). Therefore, it can be concluded that the extraordinarily high density of the positive charge around heme 4 is responsible for the unusual increase of the electron transfer rate at high ionic strength.

In conclusion, the anomalous properties found in the kinetic studies can be partially ascribed to the influence of driving force, the influence of steric or electronic effects, and the high positive charge density around heme 4.

The ionic strength dependencies of the redox potentials of a variety of cytochromes, including cytochrome b_5 (Reid et al., 1984), cytochrome c_2 (Caffrey and Cusanovich, 1991), cytochrome *c* (Margalit and Schejter, 1973), and cytochrome c_{552} (Goldkorn and Schejter, 1976), have been studied extensively. In general, a relatively small ionic strength dependency at low ionic strengths is found. For a positively charged protein (for example, horse heart cytochrome *c*), increasing the ionic strength will result in a decrease in the redox potential up to the point where the electrostatic field of the protein is masked by counterion shielding (Margalit and Schejter, 1973). In contrast, a cytochrome with a net negative charge will have a redox potential that increases with increasing ionic strength (Reid et al., 1984). The observed ionic strength dependency was consistent with Debye-Hückel expectations. In the typical situation the ionic strength effect on the redox potential saturates at ~300 mM ionic strength (Caffrey and Cusanovich, 1991). In the case of *Dv*MF cyt c_3 the effect of ionic strength persists up to at least 1 M ionic strength and has a differential effect on the individual macroscopic and microscopic redox potentials.

TABLE 3 Solvent exposure of the relevant chemical groups of the four hemes (Higuchi et al., 1984)

Chemical Groups	Solvent exposure (Å^2)			
	Heme 1	Heme 4	Heme 2	Heme 3
18^1 CH_3	22.4	23.8	NONE	NONE
17 (hydroxyl)	12.9	19.3	6.4	16.1
17 (carbonyl)	28.6	6.4	9.6	NONE
2^1 CH_3	NONE	35.0	9.8	NONE
3^2 CH_3	40.6	32.2	NONE	NONE
7^1 CH_3	NONE	NONE	NONE	NONE
8^2 CH_3	NONE	NONE	4.0	11.2
12^1 CH_3	NONE	NONE	43.4	23.8
13 (hydroxyl)	6.4	NONE	19.3	34.3
13 (carbonyl)	NONE	NONE	22.5	8.6

In the case of all four e_i^{IV}, the microscopic redox potential increases up to ~0.5 M ionic strength, then levels off in the case of e_1^{IV} and e_4^{IV} (Fig. 3), but continues to increase in the cases of e_2^{IV} and e_3^{IV} up to 1 M ionic strength. It may be significant that hemes 2 and 3 behave similarly and distinctly from hemes 1 and 4. Judging from Fig. 5 *B*, the contributions of the electrostatic fields are negligible for hemes 2 and 3 in the fully reduced state. It follows that the electrostatic potentials cannot explain the ionic strength dependency of e_i^{IV}. Thus, it must be concluded that ionic strength-dependent steric or electronic changes must occur that alter the environments of individual hemes and result in changes in the redox potentials. Unfortunately, there are no structural data of cyt c_3 in the fully reduced state. Therefore, the elucidation of the unexpected change of the redox potentials is open for the future.

We want to indicate one interesting point in connection with the structure. The crystal structure of *Dv*MF ferricyt c_3 establishes that for hemes 1 and 4, the 3^2 and 18^1 methyl groups are oriented toward the solvent; that is, constitute the exposed heme edge. However, in the case of hemes 2 and 3, the edge containing the 8^2 and 12^1 methyls is oriented toward the molecular surface. Because of asymmetry of heme, the 7^1 methyl is positioned inside of a thioether side chain and buried relative to the 12^1 methyl. Moreover, for both hemes 2 and 3 there is a salt link between a propionate and a lysine (Higuchi et al., 1984). Table 3 presents the solvent exposure of key heme positions. As can be seen, the solvent exposures are distinctly different for hemes 1 and 4 as compared to hemes 2 and 3, and are generally similar between hemes 1 and 4 and hemes 2 and 3. This classification is the same as that found in the changes of e_i^{IV} (Fig. 3 *B*) and, furthermore, that found in the NMR chemical shift changes (Figs. 2 and 4) of the fully oxidized cyt c_3. Therefore, the heme orientation could play a role in the regulation of the ionic strength-dependent electron transfer.

This work was partially supported by Grant-in-Aid for Scientific Research of Priority Area 09235208 from the Ministry of Education, Science and Culture of Japan.

REFERENCES

Akutsu, H., J. H. Hazzard, R. G. Bartsch, and M. A. Cusanovich. 1992. Reduction kinetics of the four hemes of cytochrome c_3 from *Desulfovibrio vulgaris* by flash photolysis. *Biochim. Biophys. Acta*. 1140: 144–156.

Akutsu, H., and M. Hirasawa. 1992. Non-equivalent natures of the coordinated imidazole rings of cytochrome c_3 from *D. vulgaris* Miyazaki F as studied by ^{1}H NMR. *FEBS Lett.* 308:264–266.

Benosman, H., M. Asso, P. Bertland, T. Yagi, and J. P. Gayda. 1989. EPR study of the redox interactions in cytochrome c_3 from *Desulfovibrio vulgaris* Miyazaki. *Eur. J. Biochem.* 182:51–55.

Caffrey, M. S., and M. A. Cusanovich. 1991. The effects of surface charges on the redox potential of cytochrome c_2 from the purple phototrophic bacterium *Rhodobacter capsulatus*. *Arch. Biochem. Biophys.* 285: 227–230.

Catarino, T., M. Coletta, J. LeGall, and A. V. Xavier. 1991. Kinetic study of the reduction mechanism for *Desulfovibrio gigas* cytochrome c_3. *Eur. J. Biochem*. 202:1107–1113.

Coletta, M., T. Catarino, J. LeGall, and A. V. Xavier. 1991. A thermodynamic model for the cooperative functional properties of the tetraheme cytochrome c_3 from *Desulfovibrio gigas*. *Eur. J. Biochem.* 202: 1101–1106.

Fan, K., H. Akutsu, Y. Kyogoku, and K. Niki. 1990. Estimation of microscopic redox potentials of a tetraheme protein, cytochrome c_3 of *Desulfovibrio vulgaris*, Miyazaki F, and partial assignments of heme groups. *Biochemistry*. 29:2257–2263.

Gayda, J. P., H. Benosman, P. Bertland, C. More, and M. Asso. 1988. EPR determination of interaction redox potentials in a multiheme cytochrome: cytochrome c_3 from *Desulfovibrio desulfuricans* Norway. *Eur. J. Biochem.* 177:199–206.

Goldkorn, T., and A. Schejter. 1976. The redox potential of cytochrome *c*-552 from *Euglena gracilis*: a thermodynamic study. *Arch. Biochem. Biophys.* 177:39–45.

Haladjian, J., P. Bianco, F. Guerlesquin, and M. Bruschi. 1987. Electrochemical study of the electron exchange between cytochrome c_3 and hydrogenase from *Desulfovibrio desulfuricans* Norway. *Biochem. Biophys. Res. Commun.* 147:289–1294.

Higuchi, Y., M. Kusunoki, Y. Matsuura, N. Yasuoka, and M. Kakudo. 1984. Refined structure of cytochrome c_3 at 1.8 Å resolution. *J. Mol. Biol.* 172:109–139.

Kimura, K., Y. Nakamura, T. Yagi, and H. Inokuchi. 1979. Electrical conduction of hemoprotein in the solid phase: anhydrous cytochrome c_3 film. *J. Chem. Phys.* 70:3317–3323.

Margalit, R., and A. Schejter. 1973. Cytochrome *c*: a thermodynamic study of the relationships among oxidation state, ion-binding, and structural parameters. *Eur. J. Biochem.* 32:492–499.

Matias, P. M., C. Frazao, J. Morais, M. Coll, and M. A. Carrondo. 1993. Structure analysis of cytochrome c_3 from *Desulfovibrio vulgaris* Hildenborough at 1.9 Å resolution. *J. Mol. Biol.* 234:680–699.

Matias, P. M., J. Morais, R. Coelho, M. A. Carrondo, K. Wilson, Z. Dauter, and L. Sieker. 1996. Cytochrome c_3 from *Desulfovibrio gigas*: crystal structure at 1.8 Å resolution and evidence for a specific calcium-binding site. *Protein Sci.* 5:1342–1354.

Morimoto, Y., T. Tani, H. Okumura, Y. Higuchi, and N. Yasuoka. 1991. Effects of amino acid substitution on three-dimensional structure: an X-ray analysis of cytochrome c_3 from *Desulfovibrio vulgaris* Hildenborough at 2 Å resolution. *J. Biochem.* (*Tokyo*). 110:532–540.

Nakahara, Y., K. Kimura, and H. Inokuchi. 1977. Electrical conductivity of cytochrome *c* anhydrous film. *Chem. Phys. Lett.* 47:251–254.

Nakamura, H. 1996. Roles of electrostatic interaction in proteins. *Quart. Rev. Biophys.* 29:1–90.

Nakamura, H., and S. Nishida. 1987. Numerical calculations of electrostatic potentials of protein-solvent systems by the self consistent boundary method. *J. Phys. Soc. Jpn.* 56:1609–1622.

Niki, K., Y. Kobayashi, and H. Matsuda. 1984. Determination of macroscopic standard potentials of a molecule with a reversible *n*-consecutive one-electron transfer process. Application to a tetra-heme protein: cytochrome c_3. *J. Electroanal. Chem.* 178:333–341.

Park, J.-S., M. Enoki, A. Ohbu, K. Fan, K. Niki, H. Akutsu, and Y. Kyogoku. 1991. Properties of aromatic residues in ferricytochrome c_3 of *Desulfovibrio vulgaris* Miyazaki F studied by ^{1}H NMR. *J. Mol. Struct.* 242:343–353.

Park, J.-S., T. Ohmura, A. Katayama, T. Sagara, K. Niki, M. A. Cusanovich, and H. Akutsu. 1997. A comparison of the redox potentials of cytochrome c_3 from *Desulfovibrio vulgaris* Hildenborough with those from *D. vulgaris* Miyazaki F. Effects of amino acid substitutions on the redox potential. *J. Electroanal. Chem.* 438:231–236.

Park, J.-S., T. Ohmura, T. Sagara, K. Niki, Y. Kyogoku, and H. Akutsu. 1996. Regulation of the redox order of four hemes by pH in cytochrome c_3 from *D. vulgaris* Miyazaki F. *Biochim. Biophys. Acta*. 1293:45–54.

Pierrot, M., R. Haser, M. Frey, F. Payan, and J. P. Aster. 1982. Crystal structure and electron transfer properties of cytochrome c_3. *J. Biol. Chem.* 257:14341–14348.

Reid, L. S., M. R. Mauk, and A. G. Mauk. 1984. Role of heme propionate groups in cytochrome b_5 electron transfer. *J. Am. Chem. Soc.* 106: 2182–2185.

Sagara, T., S. Nakajima, H. Akutsu, and K. Niki. 1991. Heterogeneous electron transfer rate measurements of cytochrome c_3 at mercury electrodes. *J. Electroanal. Chem.* 279:271–282.

Saito, M., and H. Kashiwagi. 1985a. Ab initio MO study on relationships between the electronic state and out-of-plane displacement of the iron atom in four-coordinate Fe-porphine. *J. Chem. Phys.* 82:848–855.

Saito, M., and H. Kashiwagi. 1985b. Ab initio MO study on equilibrium bond distance between Fe and pyridine in bis(pyridine)(porphinato) iron for various electronic states. *J. Chem. Phys.* 82:3716–3721.

Salgueiro, C. A., D. L. Turner, J. LeGall, and A. V. Xavier. 1997. Reevaluation of the redox and redox-Bohr cooperativity in tetrahaem *Desulfovibrio vulgaris* (Miyazaki F) cytochrome c_3. *J. Biol. Inorg. Chem.* 2:343–349.

Santos, H., J. J. G. Moura, J. LeGall, and A. V. Xavier. 1984. NMR studies of electron transfer mechanisms in a protein with interacting redox center: *Desulfovibrio gigas* cytochrome c_3. *Eur. J. Biochem.* 141: 283–296.

Tabushi, I., T. Nishiya, T. Yagi, and H. Inokuchi. 1983. Kinetic study on the successive four-step reduction of cyt c_3. *J. Biochem.* (*Tokyo*). 94: 1375–1385.

Takahashi, T., H. Nakamura, and A. Wada. 1992. Electrostatic forces in two lysozymes: calculations and measurements of two histidine p*K*a values. *Biopolymers*. 32:897–909.

Turner, D. L., C. A. Salgueiro, T. Catarino, J. LeGall, and A. V. Xavier. 1994. Homotropic and heterotropic cooperativity in the tetrahaem cytochrome c_3 from *Desulfovibrio vulgaris*. *Biochim. Biophys. Acta*. 1187: 232–235.

Turner, D. L., C. A. Salgueiro, T. Catarino, J. LeGall, and A. V. Xavier. 1996. NMR studies of cooperativity in the tetrahaem cytochrome c_3 from *Desulfovibrio vulgaris*. *Eur. J. Biochem.* 241:723–731.